Brain Stimulation 12 (2019) 353–360

Contents lists available at ScienceDirect

Brain Stimulation

journal homepage: http://www.journals.elsevier.com/brain-stimulation

Individual white matter bundle trajectories are associated with deep brain stimulation response in obsessive-compulsive disorder

L.C. Liebrand [a, *], M.W.A. Caan [b], P.R. Schuurman [c], P. van den Munckhof [c], M. Figee [a], D. Denys [a, d], G.A. van Wingen [a]

[a] Amsterdam UMC, University of Amsterdam, Department of Psychiatry, Amsterdam Neuroscience, Meibergdreef 9, 1105, AZ, Amsterdam, the Netherlands
[b] Amsterdam UMC, University of Amsterdam, Department of Biomedical Engineering and Physics, Amsterdam Neuroscience, Meibergdreef 9, 1105, AZ, Amsterdam, the Netherlands
[c] Amsterdam UMC, University of Amsterdam, Department of Neurosurgery, Amsterdam Neuroscience, Meibergdreef 9, 1105, AZ, Amsterdam, the Netherlands
[d] Netherlands Institute for Neuroscience, Royal Academy of Arts and Sciences, Meibergdreef 47, 1105, BA, Amsterdam, the Netherlands

ARTICLE INFO

Article history:
Received 28 May 2018
Received in revised form
16 October 2018
Accepted 22 November 2018
Available online 27 November 2018

Keywords:
Deep brain stimulation
Diffusion MRI
Tractography
Obsessive-compulsive disorder
Treatment outcome

ABSTRACT

Background: The ventral anterior limb of the internal capsule (vALIC) is a target for deep brain stimulation (DBS) in obsessive-compulsive disorder (OCD). Conventional surgical planning is based on anatomical landmarks.
Objective/hypothesis: We hypothesized that treatment response depends on the location of the active DBS contacts with respect to individual white matter bundle trajectories. This study thus aimed to elucidate whether vALIC DBS can benefit from bundle-specific targeting.
Methods: We performed tractography analysis of two fiber bundles, the anterior thalamic radiation (ATR) and the supero-lateral branch of the medial forebrain bundle (MFB), using diffusion-weighted magnetic resonance imaging (DWI) data. Twelve patients (10 females) who had received bilateral vALIC DBS for at least 12 months were included. We related the change in OCD symptom severity on the Yale-Brown obsessive-compulsive scale (Y-BOCS) between baseline and one-year follow-up with the distances from the active contacts to the ATR and MFB. We further analyzed the relation between treatment response and stimulation sites in standard anatomical space.
Results: We found that active stimulation of the vALIC closer to the MFB than the ATR was associated with better treatment outcome ($p = 0.04$; $r^2 = 0.34$). In standard space, stimulation sites were largely overlapping between treatment (non)responders, suggesting response is independent of the anatomically defined electrode position.
Conclusion: These findings suggest that vALIC DBS for OCD may benefit from MFB-specific implantation and highlight the importance of corticolimbic connections in OCD response to DBS. Prospective investigation is necessary to validate the clinical use of MFB targeting.

Introduction

Deep brain stimulation (DBS) is an emerging treatment for treatment-refractory obsessive-compulsive disorder (OCD) with an average treatment response rate of around 60% [1]. Building on psychosurgical lesioning experience [2], DBS is often targeted at ventral capsule/ventral striatum (VC/VS) areas [3], and normalizes pathological hyperconnectivity to the prefrontal cortex (PFC) [4]. At our institute, DBS is applied within the ventral part of the anterior limb of the internal capsule (vALIC) [5], a region which is known for large inter-subject white matter (WM) tracts variability [6,7]. We

Abbreviations: ATR, anterior thalamic radiation; CBT, cognitive-behavioral therapy; CSTC, cortico-striatal-thalamo-cortical; DBS, deep brain stimulation; DWI, diffusion-weighted MRI; MDD, major depressive disorder; MFB, (supero-lateral branch of the) medial forebrain bundle; NAc, nucleus accumbens; OCD, obsessive-compulsive disorder; PFC, prefrontal cortex; SSRI, selective serotonin reuptake inhibitor; TRD, treatment-resistant depression; Y-BOCS, Yale-Brown obsessive-compulsive scale; vALIC, ventral anterior limb of the interior capsule; VC, ventral capsule; VS, ventral striatum; VTA, ventral tegmental area; WM, white matter.

* Corresponding author. Amsterdam UMC, University of Amsterdam, Department of Psychiatry, Amsterdam Neuroscience, Meibergdreef 9, 1105, AZ, Amsterdam, the Netherlands.
E-mail address: L.C.Liebrand@amc.nl (L.C. Liebrand).

https://doi.org/10.1016/j.brs.2018.11.014

hypothesized that treatment response could depend on the location of the active contacts with respect to these tracts, which is currently not accounted for in DBS target planning based on anatomical landmarks.

Earlier work using diffusion-weighted magnetic resonance imaging (DWI) data has shown that the vALIC contains two fiber bundles: the anterior thalamic radiation (ATR) and the supero-lateral branch of the medial forebrain bundle (MFB) [8]. These bundles connect the PFC to different subcortical structures. The MFB connects the PFC to the ventral tegmental area (VTA) via the nucleus accumbens (NAc), and contains dopaminergic projections from the VTA to the VS [9]. The supero-lateral branch of the MFB has been described as a DBS target for treatment-resistant depression (TRD) [10] and more recently for OCD [11], where DBS could potentially be effective through improvement of the patient's mood. On the other hand, the ATR connects the PFC to the anterior thalamus and is part of the cortico-striatal-thalamo-cortical (CSTC) network, which is dysregulated in OCD [12].

In this study, we used DWI data to determine whether vALIC DBS for OCD can benefit from specific targeting of the ATR or MFB, which could enable the optimization of DBS targeting and advance our understanding of OCD's pathophysiology. We used tractography to reconstruct the ATR and MFB, and associated the distance between these bundles and the active DBS contacts with treatment response.

Material and methods

Patients

The data for this study were collected retrospectively from patients who were routinely treated at the Academic Medical Center (AMC) in Amsterdam, The Netherlands. Data were retrieved from electronic databases and fully anonymized. Inclusion requirements for this study were the availability of a pre-operative DWI scan suitable for tractography analysis, and a Yale-Brown obsessive-compulsive scale (Y-BOCS) assessment at baseline and after 12 months of DBS. All patients were screened according to regular DBS in- and exclusion criteria for OCD, as described by Denys and colleagues [13]. In brief, patients between 18 and 65 years of age, diagnosed with primary OCD for at least 5 years with a minimum baseline Y-BOCS score of 28 were eligible for DBS if the following treatments were unsuccessful: two sessions with a selective serotonin reuptake inhibitor (SSRI) at maximum dosage for 12 weeks, one session of clomipramine for 12 weeks, one augmentation trial with an atypical anti-psychotic and an SSRI for 8 weeks, and at least 16 sessions of cognitive-behavioral therapy (CBT). Exclusion criteria were significant comorbid DSM-IV Axis I disorders (except major depressive disorder (MDD) and mild anxiety disorders), severe DSM-IV Axis II personality disorders, and clinically significant neurological and medical illnesses. An independent psychiatrist from a different hospital verified the screening.

We started DBS for OCD in 2005. From 2009 onwards, DWI scans suitable for tractography were obtained as part of the pre-operative MRI protocol in a subset of patients. Twelve OCD patients (10 female, age $= 38.5 \pm 12.0$ years) out of a total of 30 that underwent DBS in the timeframe 2009–2016 met the inclusion criteria for this study, as 1) they had received DBS for OCD for at least 12 months, and 2) DWI scans suitable for tractography were made before implantation. The group consisted of seven responders (with a Y-BOCS score decrease $\geq 35\%$) and five non-responders. Demographic data are presented in Table 1. In accordance with the Dutch Medical Research Involving Human Subjects Act (WMO), the medical ethics committee of the AMC (Amsterdam, The Netherlands) waived the evaluation of this retrospective study with anonymized data, as well as the requirement to obtain informed consent.

DBS surgery

3T MRI scans were made to assess surgical eligibility at baseline. On the morning of surgery, a stereotactic frame was attached to the patient's head under general anesthesia, before scanning the patient in a 1.5T MRI scanner. Surgical planning was performed according to standard stereotactic procedures described in detail by Van den Munckhof and colleagues [5]. In short, the 3T scan and stereotactic 1.5T scan were co-registered with SurgiPlan (Elekta AB, Stockholm, Sweden) to enable planning in the stereotactic space. Target planning started with standard stereotactic coordinates relative to intercommissural line: 7 mm lateral of the midline, 3 mm anterior to the anterior border of the anterior commissure, and 4 mm inferior to the intercommissural line. Target planning was subsequently optimized, i.e, direct target planning based on representation of the nucleus accumbens and ALIC, in such way that the deepest contact of the quadripolar electrode (contact 0) was targeted in the nucleus accumbens and the upper three contacts (contacts 1–3) in the vALIC. Target coordinates were expressed in stereotactic space. Electrodes (model 3389 with 1.5 mm contacts and 0.5 mm interspace, Medtronic, Minneapolis, MN, USA) were implanted bilaterally with a sagittal angle of $\pm 75^{\circ}$ to the intercommissural line, and a coronal angle approximately following the ALIC into the NAc.

DBS treatment

The DBS device was activated two weeks after implantation, with the two middle electrode contact points (contacts 1 and 2) bilaterally activated at 3.5 V, 130 Hz, 90 μs, double unipolar stimulation. This marked the start of the optimization phase, during which the voltage was increased stepwise and clinically evaluated (bi)weekly. In the case of insufficient response after increasing the voltage, other (combinations of) electrode contact points were activated, and the process was repeated. For some patients, the stimulation's pulse width and frequency were altered with the aim of reducing side effects (e.g., agitation) or increasing the therapeutic effect. The duration of the optimization phase varied a lot between patients and lasted approximately 6 months on average. After the optimization phase, the stimulation parameters were kept constant and the patients received CBT.

Since we know from prior work that symptoms reduce further after CBT [13,14], we opted to evaluate treatment outcome when stimulation settings were stable and (the majority of) patients had received a least one course of CBT of approximately 24 weeks. Based on these criteria and the availability of 12 months follow-up data, we chose the Y-BOCS score obtained 12 months after surgery to evaluate treatment efficacy. The treatment response in our sample ranged between a 70% decrease and a 20% increase in Y-BOCS scores (see Table 1). While some patients classified as non-responders appeared to be partial responders with a Y-BOCS score decrease of up to 33%, others did not experience any symptom improvement at all. Due to the fluctuating nature of OCD symptom scores, it may not be surprising that one of the patients even had a higher Y-BOCS score after starting DBS treatment.

Imaging

We used 3T structural MRI and DWI data to reconstruct the ATR and MFB, and merged the results with the post-operative computed tomography scan that visualizes the DBS electrode position. The distance from the active stimulation site relative to the

Table 1
Patient demographics with Y-BOCS scores at baseline and follow-up and DBS settings.

Age at inclusion (years)	Gender	Y-BOCS baseline	Y-BOCS follow-up	Response (% Y-BOCS change)	DBS active contacts 0: bottom; 1: lower mid; 2: upper mid; 3: top	Voltage (V)	Frequency (Hz)	Pulse duration (μs)
47	F	36	17	−53%	1,2	5.1	130	90
37	M	28	13	−54%	2,3	5.0	130	90
25	M	29	26	−10%	0,1,2	5.8	130	90
32	F	33	10	−70%	1,2	4.4	130	90
48	F	25	30	20%	1,2	3.5	130	90
33	F	35	13	−63%	1,2	3.5	130	90
52	F	37	22	−41%	1,2	4.0	130	90
35	F	30	20	−33%	1,2	5.5	130	90
31	F	36	11	−69%	1,2	5.0	130	150
64	F	40	12	−70%	1,2	3.5	180	130
23	F	32	23	−28%	1,2	4.7	150	130
35	F	31	25	−19%	1,2	3.8	130	60

ATR and the MFB was computed, and associated with the change in the Y-BOCS score due to DBS treatment. We also compared the anatomical locations of stimulation in standard space without DWI to ascertain that treatment response is bundle dependent.

All scans were routinely made according to clinical protocols. The 3T scans were made at baseline (T = −1), 2–3 weeks prior to surgery, and included T_1-and T_2-weighted structural scans, as well as a diffusion-weighted scan. Post-surgery, a low-dose CT scan with a resolution of $0.46 \times 0.46 \times 2.0\ mm^3$ was made to confirm electrode placement. For a complete overview, see the timeline in Fig. 1A.

The 3T scans were made on a Philips Ingenia scanner (Philips Medical Systems, Best, The Netherlands), equipped with a 16-channel phased array head coil. Imaging parameters for the structural scans varied slightly over the inclusion period, and were as follows. The T_1-scans were acquired in 3D with a resolution of 0.5–1.0 mm in-plane and slices of 0.9–1.2 mm thick. The T_2-weighted scans had a slice-wise acquisition with an in-plane resolution of 0.4–0.5 mm and slice thickness of 2.0–3.3 mm. The standard clinical protocol for the acquisition of the diffusion-weighted images was changed after seven patients, which means that there are two slightly differing sets of scanning parameters. Both protocols used a 2D Stejskal-Tanner spin-echo sequence [15]. The scans had a resolution of 1.8×1.8 x $3.0/2.0 \times 2.0 \times 2.0\ mm^3$, TE = 94/92 ms, and TR = 6740/7861 ms, with 32/30 vol with a diffusion-weighting of b = 1000 s/mm^2 and one b_0-reference volume. To prevent the difference in diffusion acquisitions from having an effect on tractography results, intermediate (pre)processing steps were visually inspected, and the results of statistical analysis were corrected for acquisition type.

Image analysis pipeline

The image analysis pipeline was developed with the goal of identifying the electrode contact point coordinates relative to the MFB and ATR. To reduce the effects of different spatial resolutions, varying levels of anatomical detail and different levels of distortion, special care has been taken to ensure robust co-registrations and resampling of data. A schematic overview of the pipeline is given in Fig. 1B. After brain extraction with ANTS (Advanced Normalization Toolbox, version 2.1.0, http://stnava.github.io/ANTs/), the T_1-and T_2-weighted scans were linearly co-registered with FSL's (FMRIB Software Library, version 5.0.10, https://fsl.fmrib.ox.ac.uk/) flirt. Subsequently, registration parameters between diffusion and structural space were calculated with ANTS symmetric diffeomorphic image registration [16]. Since CT scans are not spatially distorted, the CT scans were co-registered to the structural MRI scans via a rigid transformation (ANTS), after the non-brain parts of the CT scan were removed with a custom Matlab 2014b (The Mathworks, Natick, MA) script. Individual tractography seed ROIs were drawn in the ATR and MFB in the anterior thalamic nucleus and ventral tegmental area respectively, based on Coenen et al. (2012). Additional waypoint seeds were drawn in the vALIC. All seeds were drawn in structural space and transformed to diffusion space prior to tractography.

Diffusion preprocessing and tractography

Diffusion preprocessing consisted of correcting for eddy currents and motion artifacts by affinely co-registering all diffusion-weighted volumes to the b_0 reference volume with FSL. The orientation of the b-vectors was updated accordingly [17]. Subsequently, the data were noise filtered with an adaptive LMSSE-filter that was implemented in Matlab [18]. To ensure data uniformity in the subsequent stages of analysis and because most tracking algorithms perform better with isotropic voxel sizes [19,20], the data were resampled into an isotropic 2 mm resolution. Finally, voxel-wise diffusion orientation estimates were extracted with FSL's Bedpostx [21]. Probabilistic tractography was carried out with FSL's probtrackx, with the aforementioned seeds. Tracking parameters were mostly default (5000 samples; curve threshold = 0.2; max. steps = 2500; 0.5 mm step length). The tracking results were visually inspected before and after transformation to structural space to ensure that there were no systematic differences between the two diffusion acquisitions.

Distance calculation and group level analysis

In order to preserve the individual spatial relationship between bundles and electrodes, tractography results were analyzed in subject space. Since all electrodes were identical, we performed group level analyses in a common space centered around the electrode as described below. Using this procedure, we maintained the neuroimaging data in subject space, while the analyses were performed in the common 'electrode-space'. This is schematically depicted in Fig. 2. All electrodes are oriented approximately along the inferior-superior direction within the brain, so that the axial slices centered around the electrodes can be related to a fixed depth along the electrode (Fig. 2B). Aligning these slices while preserving the transversal orientations enabled a direct comparison of tractography results between subjects.

We calculated the relative distance from the electrode to the MFB and ATR to determine which bundle was closer to the active stimulation. The relative distance was defined as $\Delta\vec{d} = \vec{d}_{MFB} - \vec{d}_{ATR}$,

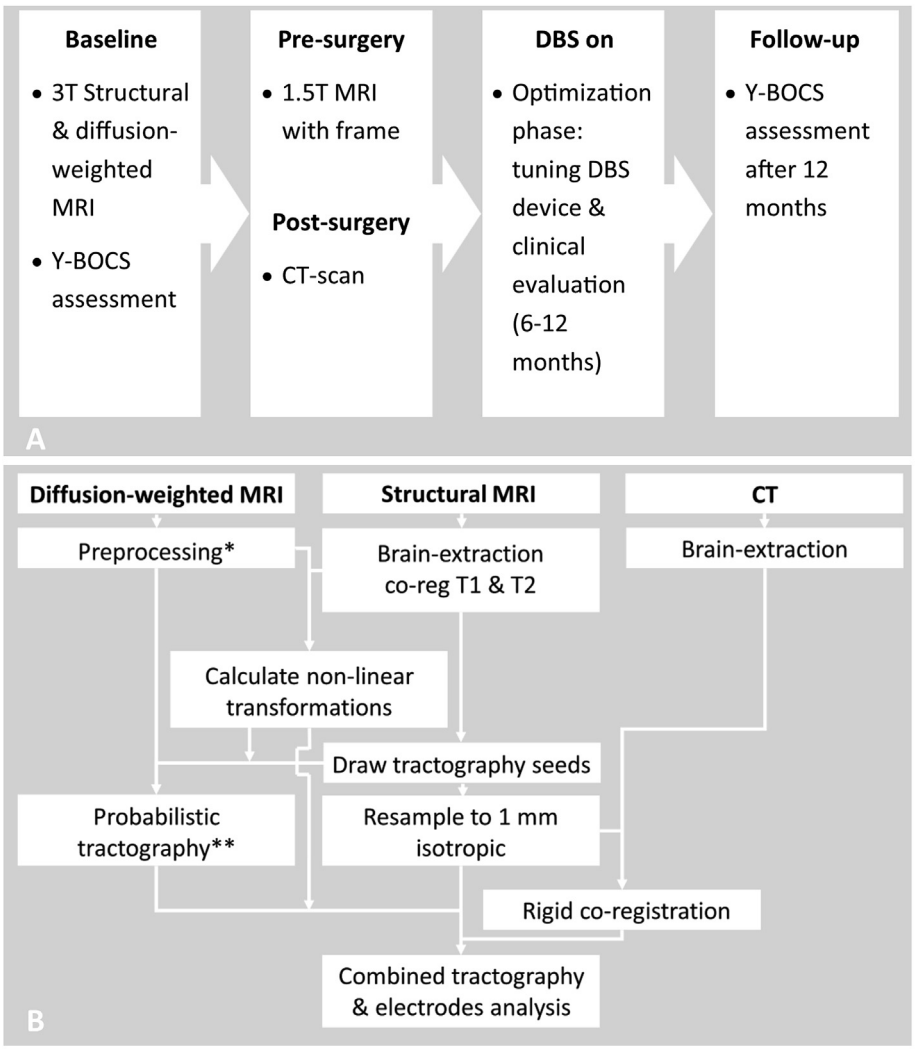

Fig. 1. Schematic overview of the treatment timeline and analysis pipeline. Panel (A) depicts a timeline showing phases of the DBS treatment that are important to this study. In (B), a schematic overview of image (pre)processing steps is shown. Note that diffusion preprocessing (*) and probabilistic tractography (**) consist of multiple smaller steps that are combined in this schematic for brevity.

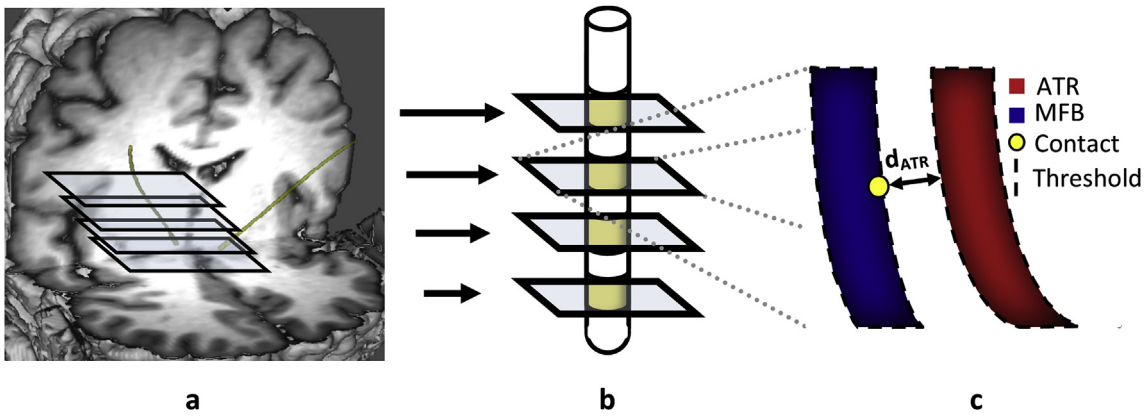

Fig. 2. Overview of distance calculation from bundles to DBS contacts. A) A 3D reconstruction of the electrodes (yellow) within a patient's brain, along with four example axial slices which are centered around one electrode. B) Since each patient was implanted with the same electrode model, these slices can be compared on a group level by overlaying the electrodes. C) Schematic overview of the distance calculation between the active contact (yellow) and the ATR (red) and MFB (blue) along the electrode axis. Distances are calculated in 3D from the contact to the closest point where the bundle exceeds the threshold. Here, $d_{MFB} = 0$ and $\Delta d < 0$. (For interpretation of the references to colour in this figure legend, the reader is referred to the Web version of this article.)

where $\overline{d}$ signifies the left-right average. The individual distances between the electrode and the bundles $\overline{d}_{MFB}$ and $\overline{d}_{ATR}$ were calculated between the active contact and the closest part of the bundle (Fig. 2C). All distances were computed based on normalized and thresholded tract probability maps. The threshold level was heuristically set to 18%, at which value the distribution of distances over subjects between contacts and bundles was optimal. Note that the relative distance is relatively invariant to this threshold level. The distances between the active contact points and the thresholded bundles were calculated in 3D with a custom Matlab script using the distance transform from the dip image toolbox (version 2.4.1, http://www.diplib.org/). Since subjects were stimulated at more than one contact, the shortest distance was chosen for the analysis.

Statistical analysis

We calculated Pearson's correlation between the relative distances $\Delta\overline{d}$ and the percentage change in Y-BOCS score to investigate their possible relationship. To correct for possible effects of using two different DWI acquisition types, we additionally performed linear regression with the sequence type as covariate.

Stimulation site heat map

To assess whether the anatomical positioning of DBS electrodes was different between responders and non-responders, we performed an additional analysis without using the information provided by DWI. We generated a heat map of treatment (non-) responders by combining the previously identified active contact sites of all patients in MNI-space (Montreal Neurological Institute), based on nonlinear transformation parameters that were calculated between each individual's T1-scan and a brain template with ANTS. In this way, it was possible to assess whether differences in treatment outcome depend on stimulation location with respect to anatomical landmarks, or bundle trajectories alone.

Results

Group level results: distance from bundles to active contacts

We first identified the ATR and supero-lateral branch of the MFB in both hemispheres for all subjects and located their positions with respect to the implanted electrodes. According to surgical planning, the electrode tips were located ventrally to the WM bundles in the NAc and the active contacts were located within the vALIC. For most subjects, there was a distinct medial-lateral organization of, respectively, the ATR and MFB within the vALIC. The electrodes were targeted to pass through the lateral part of the vALIC, which for most subjects coincided with a more proximate MFB. Next, we associated the difference in distances from the MFB and ATR to the closest active contact points to the percentage change in Y-BOCS score between baseline and one year follow-up. This analysis showed a significant positive correlation ($p = 0.04$; $r^2 = 0.34$), indicating that treatment response was better when the active contact was closer to the MFB and more distant to the ATR. After correcting for different DWI scanning sequences the result remained significant ($p = 0.02$). To ensure the results were not due to outliers, we conducted a non-parametric Spearman's rank correlation. This analysis has reduced power, but still returned a correlation at trend level ($r = 0.54$, $p = 0.07$). The results are illustrated in Fig. 3. For illustration, axial and coronal views of the tractography around the electrodes' active stimulation depth for a responder and non-responder are shown in Fig. 4. The responder is stimulated closer to the MFB than the ATR, and vice-versa for the non-responder. A complete overview of axial slices of all patients ordered by treatment response is shown in Fig. 5.

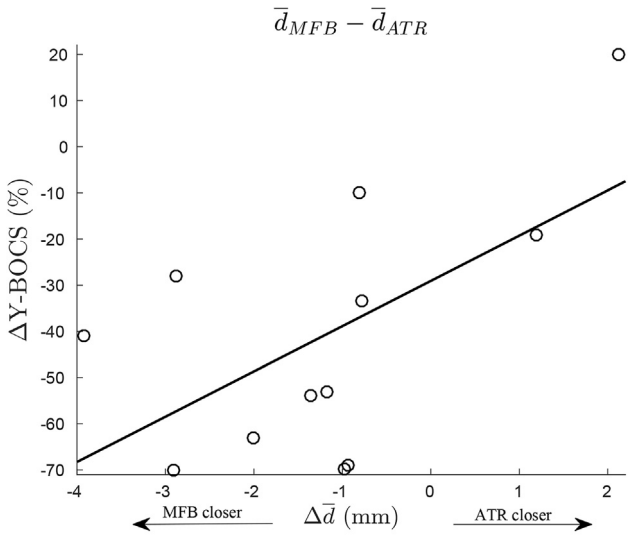

Fig. 3. Correlation of change in Y-BOCS with difference in distance from DBS contacts to ATR and MFB trajectories. Patient (N = 12) treatment response (ΔY-BOCS) plotted vs. the difference in distance in mm from contact to MFB and contact to ATR, $\Delta\overline{d}$. There is a significant correlation ($p = 0.04$, $r^2 = 0.34$; $p = 0.02$ after correcting for different scanning sequences), which is indicated with the line. Stimulation closer to the MFB seems to suggest a better treatment response (larger decrease in Y-BOCS).

Stimulation heat map

To determine whether treatment responders and non-responders could also be distinguished without knowledge of white matter bundle orientations, we created a heat map of active contact point positions in standard anatomical space, which is shown in Fig. 6. There is a large overlap within and between groups, with all stimulation sites in approximately the same location within the vALIC. This indicates that the anatomical location of the DBS electrodes does not differentiate treatment responders from non-responders.

Discussion

The aim of this study was to determine whether vALIC DBS for OCD could benefit from specific targeting of the supero-lateral branch of the MFB or ATR. We performed fiber tractography to investigate the potential relationship between bundle trajectories and stimulation sites. Through comparison of distances from the active contacts to both bundles for all patients, we found that stimulation closer to the MFB is significantly correlated with better treatment response, while there was no apparent relationship between treatment response and location of stimulation with respect to anatomical landmarks. These results may be relevant for future DBS surgical planning and targeting in OCD, but they may also help elucidating underlying mechanisms of DBS for OCD.

Our main finding suggests that targeting the MFB would be beneficial to improve treatment efficacy, even though stimulation may reach beyond the MFB. DBS specifically targeted at the MFB has already gained some interest as therapy for TRD [22], whereas specific targeting of the MFB for OCD is in its infancy [11]. Based on this study it is not possible to determine the optimal location to stimulate the supero-lateral branch of the MFB. The patients described in this study received DBS in the vALIC based on anatomical landmarks, and as such are not directly comparable to

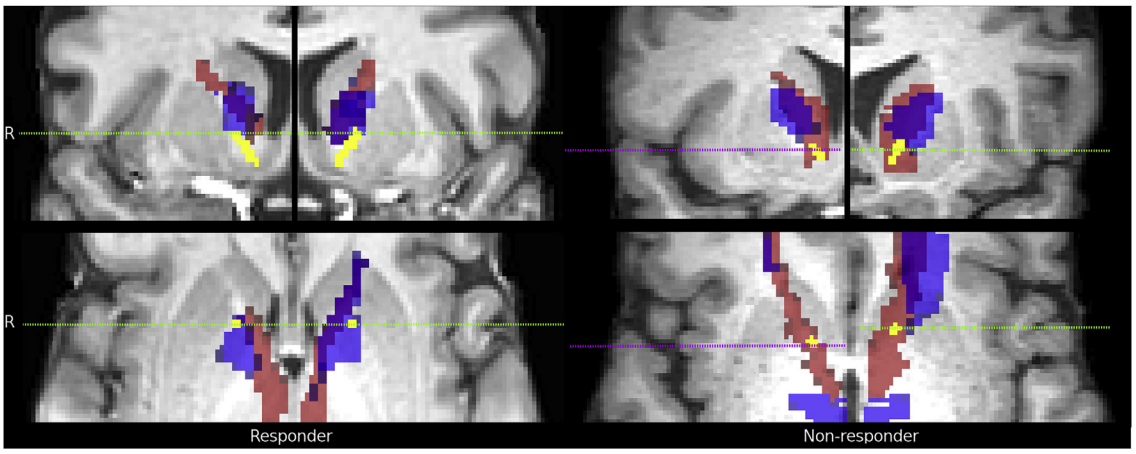

Fig. 4. Comparison of bundle trajectories around the active DBS contacts between a treatment responder and non-responder. Coronal (top) and axial (bottom) views with tractography results of the MFB (blue) and ATR (red) along with the electrodes (yellow) for a responder and non-responder. The dashed lines indicate the position of the orthogonal slice at the depth of stimulation. Note that the left electrode of the non-responder is anteriorly situated relative to the right electrode, so that the coronal view of the left hemisphere is anterior to the right hemisphere (green vs. magenta dashed lines). (For interpretation of the references to colour in this figure legend, the reader is referred to the Web version of this article.)

patients receiving MFB-specific DBS near the VTA. Further research is necessary to determine the efficacy of MFB-targeted DBS in the vALIC as opposed to near the VTA, although the use of tractography-informed stimulation in both anatomical locations seems warranted.

Considering the prevalence of comorbid depression in treatment-resistant OCD patients [13,23], it is possible that stimulation of the MFB initiates a therapeutic effect in OCD through an improvement in mood similar to MFB DBS for TRD. This is supported by clinical observations that suggest that DBS initially

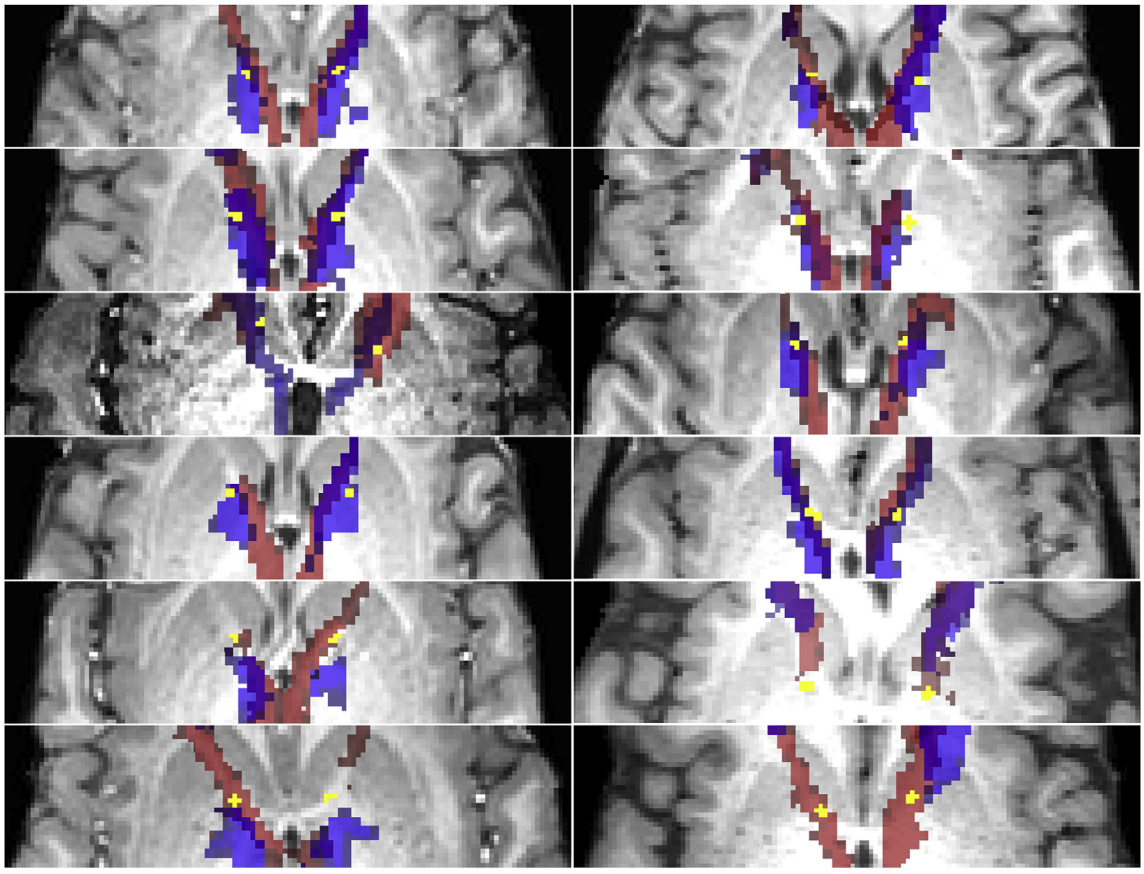

Fig. 5. Electrode and tractography overview of all patients. Axial slices showing tractography results of the MFB (blue) and ATR (red) around the electrodes (yellow) for all patients included in this study. The slices are ordered (top-bottom) based on treatment response, with the best treatment response at the top. In the top slices the electrodes appear to be more proximate to the MFB, whereas in the lower slices the ATR seems closer. (For interpretation of the references to colour in this figure legend, the reader is referred to the Web version of this article.)

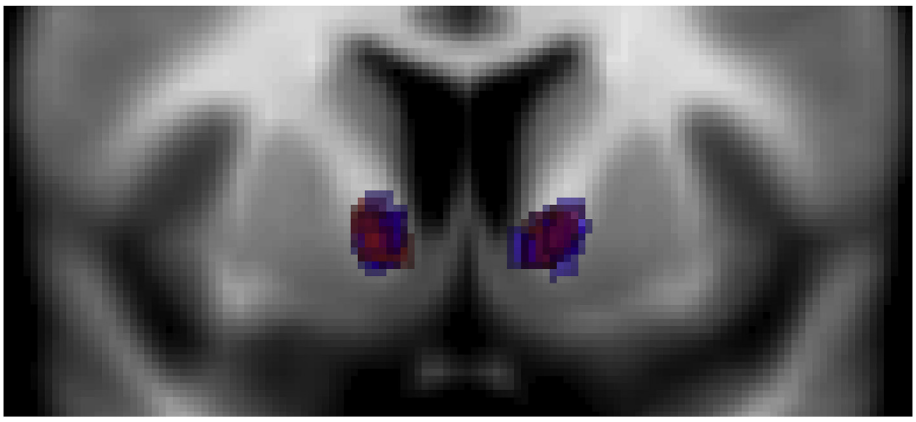

Fig. 6. Comparison of stimulation sites in standard anatomical space. Coronal slice of a T1-scan in MNI-space overlaid with two heat maps showing active contact sites for all 12 patients, with treatment responders in blue and non-responders in red. All active contacts are situated in the white matter (vALIC), with a large overlap within and between groups. (For interpretation of the references to colour in this figure legend, the reader is referred to the Web version of this article.)

improves mood and anxiety [24], in advance of long-term recovery of compulsive symptoms through CBT [13,14]. Within OCD pathophysiology, it would seem that the MFB is mainly responsible for the depressed mood and anxiety associated with obsessions, and stimulation of the MFB would indirectly increase the patients' ability to cope with and challenge compulsive behavior. Nonetheless, our results do not provide evidence on whether pathological MFB connectivity is responsible for OCD in the first place, or that the improvement in mood and anxiety due to MFB stimulation merely acts as a catalyst for CBT targeted at compulsivity, since we have not looked into the effect of stimulation and CBT separately.

The limited role of the ATR in the efficacy of DBS for OCD could be considered surprising, as the ATR connects different brain structures within the CSTC network that are at the core of the pathophysiological model of OCD [25]. The more prominent role for the MFB supports more recent models of OCD that acknowledge the importance of additional affective networks [12,26,27]. Nevertheless, these networks may interact at the level of the striatum, as the MFB connects the striatum, PFC and VTA. Therefore, the MFB could influence the CSTC at different locations within the network, which may be necessary to enable normalization of CSTC activity for these otherwise refractory patients [4,28].

Limitations of this work include the small number of subjects ($N = 12$). Even though statistical power was sufficient to detect associations between white matter trajectories and clinical outcome, small sample sizes limit the generalizability of the results. In order to avoid the potential influence of outliers in our small sample, we conducted a non-parametric Spearman's rank correlation. This correlation coefficient was highly comparable to the parametric Pearson's correlation but the significance level was slightly lower, which we attribute to the lower statistical power in non-parametric vs. parametric tests. Our sample was considerable given the limited number of patients that underwent DBS for OCD and completed pre-surgical DWI scanning. Regardless, future studies should aim to replicate these results with more subjects.

A second limitation is the use of two different diffusion sequences that originated from an update in clinical scanning protocols over the inclusion period. After correction for sequence differences (by including a covariate for the different sequence types) the results remained significant ($p = 0.02$), indicating that the results are robust with respect to sequence type. Another limitation lies within the use of tractography. Tractography is a powerful tool that can be used to optimize existing targeting procedures [29], or provide a rationale for hitherto untested DBS targets [10]. However, one must take care when interpreting tracking results, since tractography is not an exact reconstruction of WM pathways and trajectories may vary with the tracking algorithm's parameters. Furthermore, diffusion-weighted scans are susceptible to imaging artifacts and results may be dependent on the quality of data (pre-)processing. To minimize the influence of these factors, we used robust preprocessing strategies and probabilistic tractography [30].

Future work should focus on prospective testing of MFB-targeted stimulation by incorporating tractography information into surgical planning and DBS optimization, which may increase treatment response and shorten the time to optimize stimulation settings.

Conclusions

In this retrospective study, we have shown that active stimulation of the vALIC closer to the supero-lateral branch of the MFB than the ATR is related to a better outcome for treatment-refractory OCD. It is possible that stimulation of the affective circuitry is responsible for this treatment effect, similar to antidepressant effects of MFB DBS for TRD. Tractography-assisted targeting of the MFB inside the vALIC could lead to improved treatment response, which needs to be tested in a prospective study.

Conflicts of interest

Dr. Caan is shareholder of Nico-lab BV. The other authors declare no competing financial interests.

Acknowledgments

Funding: This study was supported by an Innovation Impulse grant (#2015.011) from the Academic Medical Center.

Appendix A. Supplementary data

Supplementary data to this article can be found online at https://doi.org/10.1016/j.brs.2018.11.014.

References

[1] Alonso P, Cuadras D, Gabriëls L, Denys D, Goodman W, Greenberg BD, et al. Deep brain stimulation for obsessive-compulsive disorder: a meta-analysis of treatment outcome and predictors of response. PLoS One 2015;10:1–16. https://doi.org/10.1371/journal.pone.0133591.

[2] Tierney TS, Abd-El-Barr MM, Stanford AD, Foote KD, Okun MS. Deep brain stimulation and ablation for obsessive compulsive disorder: evolution of contemporary indications, targets and techniques. Int J Neurosci 2014;124:394–402. https://doi.org/10.3109/00207454.2013.852086.
[3] Greenberg BD, Gabriels LA, Malone DA, Rezai AR, Friehs GM, Okun MS, et al. Deep brain stimulation of the ventral internal capsule/ventral striatum for obsessive-compulsive disorder: worldwide experience. Mol Psychiatr 2010;15:64–79. https://doi.org/10.1038/mp.2008.55.
[4] Figee M, Luigjes J, Smolders R, Valencia-Alfonso C-E, van Wingen G, de Kwaasteniet B, et al. Deep brain stimulation restores frontostriatal network activity in obsessive-compulsive disorder. Nat Neurosci 2013;16:386–7. https://doi.org/10.1038/nn.3344.
[5] Munckhof P, Bosch DA, Mantione MHM, Figee M, Denys DAJP, Schuurman PR. Active stimulation site of nucleus accumbens deep brain stimulation in obsessive–compulsive disorder is localized in the ventral internal capsule. In: Stereotact. Funct. Neurosurg, vol. 117. Vienna: Springer Vienna; 2013. p. 53. https://doi.org/10.1007/978-3-7091-1482-7_9.
[6] Makris N, Rathi Y, Mouradian P, Bonmassar G, Papadimitriou G, Ing WI, et al. Variability and anatomical specificity of the orbitofrontothalamic fibers of passage in the ventral capsule/ventral striatum (VC/VS): precision care for patient-specific tractography-guided targeting of deep brain stimulation (DBS) in obsessive compulsive. Brain Imag Behav 2016;10:1054–67. https://doi.org/10.1007/s11682-015-9462-9.
[7] Nanda P, Banks GP, Pathak YJ, Sheth SA. Connectivity-based parcellation of the anterior limb of the internal capsule. Hum Brain Mapp 2017;00. https://doi.org/10.1002/hbm.23815.
[8] Coenen VA, Panksepp J, Hurwitz TA, Urbach H, Mädler B. Human medial forebrain bundle (MFB) and anterior thalamic radiation (ATR): imaging of two major subcortical pathways and the dynamic balance of opposite affects in understanding depression. J Neuropsychiatry Clin Neurosci 2012;24:223–36. https://doi.org/10.1176/appi.neuropsych.11080180.
[9] Haber SN, McFarland NR. The concept of the ventral striatum in nonhuman primates. Ann N Y Acad Sci 1999;877:33–48. https://doi.org/10.1111/j.1749-6632.1999.tb09259.x.
[10] Schlaepfer TE, Bewernick BH, Kayser S, Mädler B, Coenen VA. Rapid effects of deep brain stimulation for treatment-resistant major depression. Biol Psychiatry 2013;73:1204–12. https://doi.org/10.1016/j.biopsych.2013.01.034.
[11] Coenen VA, Schlaepfer TE, Goll P, Reinacher PC, Voderholzer U, Tebartz van Elst L, et al. The medial forebrain bundle as a target for deep brain stimulation for obsessive-compulsive disorder. CNS Spectr 2016;22:282–9. https://doi.org/10.1017/S1092852916000286.
[12] van den Heuvel OA, van Wingen G, Soriano-Mas C, Alonso P, Chamberlain SR, Nakamae T, et al. Brain circuitry of compulsivity. Eur Neuropsychopharmacol 2016;26:810–27. https://doi.org/10.1016/j.euroneuro.2015.12.005.
[13] Denys D, Mantione M, Figee M, van den Munckhof P, Koerselman F, Westenberg H, et al. Deep brain stimulation of the nucleus accumbens for treatment-refractory obsessive-compulsive disorder. Arch Gen Psychiatr 2010;67:1061. https://doi.org/10.1001/archgenpsychiatry.2010.122.
[14] Mantione M, Nieman DDH, Figee M, Denys D. Cognitive–behavioural therapy augments the effects of deep brain stimulation in obsessive–compulsive disorder. Psychol Med 2014;44:3515–22. https://doi.org/10.1017/S0033291714000956.
[15] Stejskal EO, Tanner JE. Spin diffusion measurements: spin echoes in the presence of a time-dependent field gradient. J Chem Phys 1965;42:288–92. https://doi.org/10.1063/1.1695690.
[16] Avants BB, Epstein CL, Grossman M, Gee JC. Symmetric diffeomorphic image registration with cross-correlation: evaluating automated labeling of elderly and neurodegenerative brain. Med Image Anal 2008;12:26–41. https://doi.org/10.1016/j.media.2007.06.004.
[17] Leemans A, Jones DK. The B-matrix must be rotated when correcting for subject motion in DTI data. Magn Reson Med 2009;61:1336–49. https://doi.org/10.1002/mrm.21890.
[18] Caan M, Khedoe G, Poot D, Den Dekker A, Olabarriaga S, Grimbergen K, et al. Adaptive noise filtering for accurate and precise diffusion estimation in fiber crossings. Lect Notes Comput Sci (Including Subser Lect Notes Artif Intell Lect Notes Bioinformatics) 2010;6361. https://doi.org/10.1007/978-3-642-15705-9_21. LNCS:167–74.
[19] Basser PJ, Pajevic S, Pierpaoli C, Duda J, Aldroubi A. In vivo fiber tractography using DT-MRI data. Magn Reson Med 2000;44:625–32. https://doi.org/10.1002/1522-2594(200010)44:4<625::AID-MRM17>3.0.CO;2-O.
[20] Mukherjee P, Chung SW, Berman JI, Hess CP, Henry RG. Diffusion tensor MR imaging and fiber tractography: technical considerations. Am J Neuroradiol 2008;29:843–52. https://doi.org/10.3174/ajnr.A1052.
[21] Behrens TEJ, Berg HJ, Jbabdi S, Rushworth MFS, Woolrich MW. Probabilistic diffusion tractography with multiple fibre orientations: what can we gain? Neuroimage 2007;34:144–55. https://doi.org/10.1016/j.neuroimage.2006.09.018.
[22] Bewernick BH, Kayser S, Gippert SM, Switala C, Coenen VA, Schlaepfer TE. Deep brain stimulation to the medial forebrain bundle for depression- long-term outcomes and a novel data analysis strategy. Brain Stimul 2017;10:664–71. https://doi.org/10.1016/j.brs.2017.01.581.
[23] Greenberg BD, Malone DA, Friehs GM, Rezai AR, Kubu CS, Malloy PF, et al. Three-year outcomes in deep brain stimulation for highly resistant obsessive-compulsive disorder. Neuropsychopharmacology 2006;31:2384–93. 1301165 [pii]\r10.1038/sj.npp.1301165.
[24] de Koning PP, Figee M, Endert E, van den Munckhof P, Schuurman PR, Storosum JG, et al. Rapid effects of deep brain stimulation reactivation on symptoms and neuroendocrine parameters in obsessive-compulsive disorder. Transl Psychiatry 2016;6:e722. https://doi.org/10.1038/tp.2015.222.
[25] Ahmari SE, Spellman T, Douglass NL, Kheirbek MA, Simpson HB, Deisseroth K, et al. Repeated cortico-striatal stimulation generates persistent OCD-like behavior. Science 2013;340:1234–9. https://doi.org/10.1126/science.1234733. 80-.
[26] Milad MR, Rauch SL. Obsessive-compulsive disorder: beyond segregated cortico-striatal pathways. Trends Cognit Sci 2012;16:43–51. https://doi.org/10.1016/j.tics.2011.11.003.
[27] Wood J, Ahmari SE. A framework for understanding the emerging role of corticolimbic-ventral striatal networks in OCD-associated repetitive behaviors. Front Syst Neurosci 2015;9:1–22. https://doi.org/10.3389/fnsys.2015.00171.
[28] Figee M, De Koning P, Klaassen S, Vulink N, Mantione M, Van Den Munckhof P, et al. Deep brain stimulation induces striatal dopamine release in obsessive-compulsive disorder. Biol Psychiatry 2014;75:647–52. https://doi.org/10.1016/j.biopsych.2013.06.021.
[29] Riva-Posse P, Choi KS, Holtzheimer PE, Crowell AL, Garlow SJ, Rajendra JK, et al. A connectomic approach for subcallosal cingulate deep brain stimulation surgery: prospective targeting in treatment-resistant depression. Mol Psychiatr 2017:1–7. https://doi.org/10.1038/mp.2017.59.
[30] Jones DK, Cercignani M. Twenty-five pitfalls in the analysis of diffusion MRI data. NMR Biomed 2010;23:803–20. https://doi.org/10.1002/nbm.1543.